Title

Acute Lesioning and Rapid Repair of Hypothalamic Neurons outside the Blood-Brain Barrier



Journal

Cell Reports, 19(11)

ISSN

2639-1856

Authors

Yulyaningsih, Ernie

Rudenko, Ivan A

Valdearcos, Martin

et al.

Publication Date

2017-06-01

DOI

10.1016/j.celrep.2017.05.060

Peer reviewed

HHS Public Access

Author manuscript

*Cell Rep*. Author manuscript; available in PMC 2017 October 22.

Published in final edited form as:

*Cell Rep*. 2017 June 13; 19(11): 2257–2271. doi:10.1016/j.celrep.2017.05.060.

# Acute lesioning and rapid repair of hypothalamic neurons outside the blood-brain barrier

**Ernie Yulyaningsih**[1], **Ivan A. Rudenko**[1], **Martin Valdearcos**[1], **Emma Dahlén**[1], **Eirini Vagena**[1], **Alvin Chan**[1], **Arturo Alvarez-Buylla**[2], **Christian Vaisse**[1,3], **Suneil K. Koliwad**[1,3], and **Allison W. Xu**[1,4,*]

[1]Diabetes Center, University of California, San Francisco, San Francisco, CA 94143, USA

[2]Eli and Edythe Broad Center of Regeneration Medicine, University of California, San Francisco, San Francisco, CA 94143, USA

[3]Department of Medicine, University of California, San Francisco, San Francisco, CA 94143, USA

[4]Department of Anatomy, University of California, San Francisco, San Francisco, CA 94143, USA

## Summary

Neurons expressing agouti-related protein (AgRP) are essential for feeding. The majority of these neurons are located outside the blood-brain barrier (BBB), allowing them to directly sense circulating metabolic factors. Here we show that in adult mice, AgRP neurons outside the BBB ($AgRP^{OBBB}$) were rapidly ablated by peripheral administration of monosodium glutamate (MSG), whereas AgRP neurons inside the BBB and most proopiomelanocortin (POMC) neurons were spared. MSG treatment induced proliferation of tanycytes, the putative hypothalamic neural progenitor cells, but the newly proliferated tanycytes did not become neurons. Intriguingly, $AgRP^{OBBB}$ neuronal number increased within a week after MSG treatment, and newly emerging AgRP neurons were derived from post-mitotic cells including some from the *Pomc*-expressing cell lineage. Our study reveals that the lack of protection by the BBB renders $AgRP^{OBBB}$ vulnerable to lesioning by circulating toxins, but that the rapid re-emergence of $AgRP^{OBBB}$ is part of a reparative process to maintain energy balance.

## Graphical abstract

*Lead Contact: Allison W. Xu, Diabetes Center, University of California, San Francisco, San Francisco, CA 94143. Allison.Xu@ucsf.edu.

**Author contributions**

E.Y., I.A.R., A.A., C.V., S.K.K. and A.W.X. designed the experiments. E.Y., I.A.R., M.V., E.D., E.V., A.C. performed the experiments. E.Y., I.A.R. and E.D. analyzed the data. E.Y., I.A.R., and A.W.X. wrote the manuscript. A.A., C.V. and S.K.K. edited the manuscript.

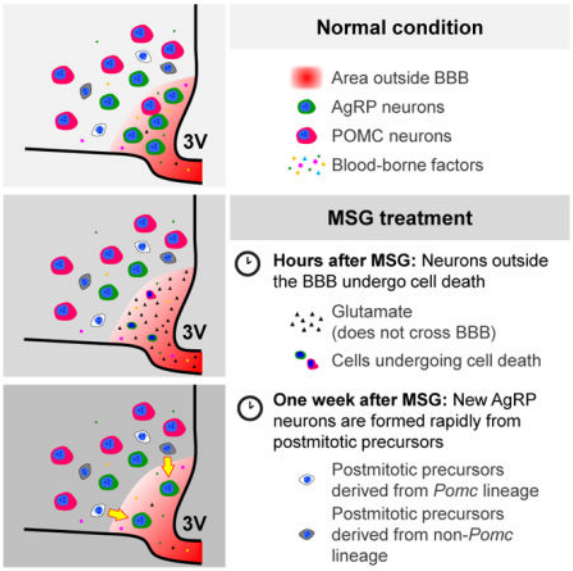


## Introduction

The ability to monitor the body's energy stores and adjust appetite and energy expenditure accordingly is essential for survival in an environment where food availability is unpredictable. A number of hypothalamic and extra-hypothalamic neuronal subgroups have been implicated in this dynamic process. Among them, neurons expressing agouti-related protein (AgRP) are unique among hypothalamic neurons due to their anatomical relationship with the blood-brain barrier (BBB). We have recently shown that 60–70% of AgRP neurons in adult mice are located outside the BBB ($AgRP^{OBBB}$), while most of the neighboring proopiomelanocortin (POMC) neurons are inside of the BBB (Olofsson et al., 2013). $AgRP^{OBBB}$ are in a position to directly sense dynamic changes in circulating leptin levels whereas hypothalamic neurons behind the BBB are less sensitive to these changes, making $AgRP^{OBBB}$ first-line responders to dynamic changes in nutritional status (Olofsson et al., 2013). Optogenetic or chemogenetic stimulation of AgRP neurons leads to voracious feeding while acute ablation of these neurons by diphtheria toxin leads to severe anorexia (Aponte et al., 2011; Krashes et al., 2011; Luquet et al., 2005). Thus, AgRP neurons are indispensable for appetite regulation and lesioning of these neurons could have severe metabolic consequences.

Although the unique anatomical location of $AgRP^{OBBB}$ affords advantages for metabolic regulation, it may also directly expose these neurons to circulating toxins or metabolites, increasing their vulnerability to damage. To date, very little is known about this potential vulnerability, or the repair mechanisms following the loss of hypothalamic neurons. In mammals, adult neurogenesis is believed to be largely restricted to the ventricular-subventricular zone (V-SVZ) of the lateral ventricles and the subgranular zone (SGZ) of the dentate gyrus in the hippocampus (Kriegstein and Alvarez-Buylla, 2009). Like the vast majority of CNS neurons, most hypothalamic neurons are born during embryogenesis (Ishii and Bouret, 2012; Werner et al., 2012). The adult hypothalamus is traditionally considered

to possess limited neurogenic activity. However, neural progenitor cells can be isolated from adult hypothalamus; they exhibit stem cell properties and differentiate *in vitro* into neurons that express hypothalamic neuropeptides (Markakis et al., 2004). Furthermore, recent studies reveal that normal adult hypothalamus has constitutive proliferative and neurogenic activities, and that hypothalamic neurons, including AgRP neurons, have high rate of spontaneous turnover in juvenile and adult hypothalamus (Kokoeva et al., 2007; McNay et al., 2012). Therefore, new neurons generated in the adult hypothalamus could potentially replenish neurons that die due to damage, e.g. $AgRP^{OBBB}$ that lack the protection of the BBB.

To investigate if $AgRP^{OBBB}$ are especially prone to lesioning, we employed a neurotoxin that circulates in the body but does not cross the BBB. Monosodium glutamate (MSG), a salt of glutamate and a common flavor-enhancer, has such properties. The BBB is impermeable to glutamate and prevents its entry into the brain (Hawkins, 2009). Thus, although glutamate levels are high in the plasma (50–100 μmol/L), its concentration is maintained at a very low level in the extracellular fluids of the brain (0.5–2 μmol/L), which is important for optimal neuronal function (Hawkins, 2009). Glutamate is an excitatory neurotransmitter and exerts excitotoxic effects at high concentrations. Indeed, injecting MSG into neonatal monkeys or rodents causes hypothalamic cell death within hours (Burde et al., 1971; Olney and Sharpe, 1969), and this strategy has been used to generate obesity models based on hypothalamic lesioning (Olney, 1969). In this study, we investigated if peripheral administration of MSG preferentially damages $AgRP^{OBBB}$ and if the brain has an innate ability to repair lesions to these neurons.

## Results

### AgRP neurons do not undergo spontaneous turnover in adult mice under basal conditions

It was reported that *de novo* neurogenesis occurs constitutively in the adult hypothalamus under normal conditions, and close to 60% of cells that incorporate bromodeoxyuridine (BrdU) at 4 months of age differentiate into neurons (Kokoeva et al., 2007; McNay et al., 2012). Moreover, a large majority of AgRP neurons labeled with BrdU during embryogenesis also undergo spontaneous turnover (McNay et al., 2012). We reasoned that $AgRP^{OBBB}$, lacking the protection of the BBB, may be even more inclined to undergo spontaneous turnover due to excess “wear and tear”. If so, constitutive neurogenesis may function to replenish these $AgRP^{OBBB}$. To investigate this, 12- to 16-week-old mice received an intracerebroventricular (i.c.v.) infusion of BrdU via osmotic minipumps, and their hypothalami were examined 4 weeks later (Figure 1A). Although abundant $BrdU^+$ cells were observed in the hypothalamus (Figure 1B), we failed to observe any $BrdU^+$ cells that co-expressed the neuronal marker HuC/D (0 out of 1,303 cells counted) (Figure 1C). Any rare cells staining positive for both HuC/D and BrdU exhibited a nuclear HuC/D staining pattern rather than the cytoplasmic pattern characteristic of neurons. Similarly, although we detected BrdU colocalization with NeuN, a mature neuronal marker, in the SGZ of the hippocampus, a known neurogenic region (Figure S1), we did not observe any NeuN-expressing $BrdU^+$ cells in the hypothalamus (0 out of 921 cells counted) (Figure 1D).

Therefore, in contrast to previous work, we failed to detect new neurons that were derived from *de novo* cell division in the hypothalamus of 12- to 16-week-old adult mice.

We next investigated whether AgRP neurons, the majority of which are not protected by the BBB, may undergo basal turnover. To do so, we utilized the *Agrp-CreER$^{T2}$*, *Ai14(tdTomato)* mouse in which tamoxifen injection induces expression of tdTomato specifically in AgRP neurons in the adult hypothalamus (Wang et al., 2014). Since tdTomato expression is controlled by the constitutive *CAG* promoter that is independent of *Npy* or *Agrp* transcriptional regulation, tdTomato, once turned on by tamoxifen, permanently marks existing AgRP neurons, allowing the fate of these neurons to be traced. Previous work shows that tamoxifen remains detectable after repeated administration and its ability to induce nuclear translocation of the Cre-ER$^{T2}$ protein could be long-lasting (Ye et al., 2015). With this consideration, mice were given a single tamoxifen administration to minimize the confounding effect of repeated tamoxifen exposure (Figure 1E). To ensure that tdTomato-expressing cells are indeed AgRP neurons, mice carrying *Agrp-CreER$^{T2}$*, *Ai14(tdTomato)* were further crossed with *Npy*-GFP reporter. Although *Npy* is expressed in many brain regions, 95% of NPY neurons in the arcuate nucleus (ARC) co-express AgRP, hence *Npy*-GFP expression can be used as a surrogate marker for AgPR neurons within the ARC (Broberger et al., 1998). Although only a subset of *Npy*-GFP neurons were labeled with tdTomato with a single subcutaneous tamoxifen injection, almost all tdTomato$^+$ cells were GFP$^+$ (922 out of 926 counted) suggesting that tdTomato expression faithfully marks AgRP neuronal lineage. With this in mind, 6- to 10-week-old *Agrp-CreER$^{T2}$*, *Ai14(tdTomato)*, *Npy-GFP* mice were given a single injection of tamoxifen, and examined following a short (10 days) or a long (32–40 weeks) chase period. Using this strategy, if AgRP neurons were to undergo turnover during the chase period, the number of tdTomato$^+$ cells would be expected to decline with time. However, the number of tdTomato$^+$ cells throughout the entire ARC did not change in the 8- to 10-month chase period (Figures 1E–F). Further, the number of cells expressing *Npy*-GFP reporter also remained unchanged during this chase period (Figure 1G). This result, together with the lack of BrdU labeling of hypothalamic neurons (above), indicates that AgRP neurons do not undergo turnover under basal condition in 2- to 10-month-old adult animals.

## Majority of bFGF-responsive cells in the adult hypothalamus reside in the V-SVZ zone and the adjacent arcuate nucleus

Since neural progenitor cells are highly responsive to growth factors, we infused basic fibroblast growth factor (bFGF) and BrdU into the lateral ventricle of 16- to 18-week-old mice via osmotic minipump for a week. bFGF infusion stimulated marked proliferation of nestin$^+$ cells in the V-SVZ of the 3$^{rd}$ ventricle (3V), and many of these nestin$^+$, BrdU$^+$ cells were found in location of α-tanycytes (Figures 2A–B). While expression of doublecortin (DCX), an immature neuronal marker, was undetectable in untreated adult hypothalamus, a marked increase in DCX signal was detected 1 week after bFGF infusion (Figures 2C–D). Despite this, no colocalization of BrdU with neuronal markers HuC/D or NeuN was observed 4–6 weeks after bFGF infusion (Figure 2E). Of note, at 1 week or 4–6 weeks after bFGF infusion into the lateral ventricle, the majority of the BrdU$^+$ cells were found near the ARC parenchyma (Figures 2E–F). Thus, although the adult hypothalamus contains cells that

proliferate in response to growth factors and express immature neuronal marker DCX, these newly proliferated cells do not appear to turn into mature neurons under these conditions.

## Peripherally administered MSG rapidly ablates AgRP$^{OBBB}$ in adult mice, but spares those inside the BBB and the majority of POMC neurons

We next investigated whether AgRP$^{OBBB}$ are vulnerable to MSG-induced lesion. We first evaluated the timeline for MSG to lesion the adult hypothalamus. Mice carrying the *Npy*-GFP reporter were subcutaneously injected with a single dose of MSG (3.5 g/kg body weight) or an isomolar sodium vehicle solution, following which the hypothalami were examined. Within 2 hours after MSG treatment, a significant reduction in AgRP cell number was observed. A number of remaining AgRP neurons exhibited pyknotic features (Figure S2). This result is consistent with previous findings that MSG treatment rapidly induces necrosis of ARC neurons within 3 hours (Abraham et al., 1971; Burde et al., 1971; Olney, 1969; Olney and Sharpe, 1969).

To assess the effects of MSG on AgRP$^{OBBB}$, mice that carried the *Npy*-GFP reporter were subcutaneously injected with vehicle or MSG. To mark cells outside the BBB, Evans Blue was injected intracardially before perfusion with fixative. In vehicle-treated mice, most AgRP neurons in the mediobasal part of the ARC were Evans Blue$^{+}$, while AgRP neurons in the lateral ARC were Evans Blue$^{-}$ (Figures 3A–B), consistent with prior observation (Olofsson et al., 2013). MSG treatment rapidly ablated AgRP neurons, most of which had been Evans Blue$^{+}$ and were located in the mediobasal ARC. By contrast, most of the AgRP neurons that were resistant to MSG treatment were located in the lateral ARC and were Evans Blue$^{-}$ (Figures 3A–B). On the other hand, only a small fraction of hypothalamic POMC neurons, identified by immunostaining against ACTH, a protein product of the *Pomc* gene, were ablated by MSG treatment (Figure S3), consistent with the notion that these neurons are predominantly located inside the BBB (Olofsson et al., 2013). Together, these results indicate that AgRP$^{OBBB}$ are vulnerable to cytotoxic ablation by peripherally administered MSG, whereas AgRP and POMC neurons located inside the BBB are protected from these effects.

## Emergence of doublecortin-expressing cells and new AgRP neurons after MSG-mediated ablation of hypothalamic neurons

Within one day of MSG-injection, two-thirds of AgRP neurons in the mediobasal compartment of the ARC were ablated, while those in the lateral ARC were relatively spared (Figures 3C–D). However subsequent monitoring over a 7-day period revealed a small but rapid rebound in the number of AgRP neurons within the mediobasal ARC (Figures 3C–D). This recovery made up approximately 28% of the lost AgRP neurons in the mediobasal ARC. Although modest, this post-ablative increase in the AgRP neuronal numbers was reproduced in 2 independent cohorts of male mice and 1 cohort of female mice. In contrast, the number of AgRP neurons in the lateral ARC did not significantly change over time after MSG treatment (Figure 3D).

These rapidly formed AgRP neurons could represent newly differentiated AgRP neurons. Alternatively, they could potentially represent preexisting AgRP neurons that, rather than

dying, transiently downregulated *Npy*-GFP reporter expression in response to MSG, but subsequently recovered this expression over the following 7 days. To differentiate between these possibilities, mice carrying *Agrp-CreER*$^{T2}$, *Ai14(tdTomato)*, *Npy-GFP* were injected with tamoxifen to label preexisting AgRP neurons. Upon tamoxifen injection, preexisting AgRP neurons become labeled with the red fluorescent tdTomato reporter under the control of the constitutive *CAG* promoter. Since these preexisting AgRP neurons will also express the green *Npy*-GFP reporter, they will appear yellow. If instead of ablating AgRP neurons, MSG-treatment simply induces a transient silencing of the *Npy*-GFP reporter, we would expect it to acutely increase the number of tdTomato$^+$, GFP$^-$ ("red only") cells in the hypothalamus. In vehicle-treated mice, a total of 547 tdTomato$^+$ cells (10 sections per mouse from 3 mice) were observed. Of these, 543 co-expressed GFP. In quantifying matching sections from 1-day MSG-treated mice, we observed a total of 57 tdTomato$^+$ cells, all of which were GFP$^+$ (10 sections per mouse from 3 mice). No tdTomato$^+$, GFP$^-$ cells ("red only" cells) was observed in 1-day MSG-treated mice (Figures 3E–G). This finding indicates that the AgRP neurons emerging following MSG-ablation do not simply reflect preexisting AgRP neurons that transiently downregulated GFP reporter expression, but instead suggests that these neurons are newly differentiated from AgRP-negative precursors.

We next examined if MSG-induced lesions lead to the appearance of cells expressing DCX, an immature neuronal marker. In control adult mice, DCX was expressed in the SGZ of the dentate gyrus (Figure S4A), the V-SVZ, the rostral migratory stream and the olfactory bulb, regions known to contain young neurons (Kriegstein and Alvarez-Buylla, 2009). However, in adult control mice, we did not observe DCX$^+$ cells in the hypothalamus (Figure S4B & S4G). Interestingly, 3 days and 1 week after MSG treatment, cells expressing DCX were observed in the ARC (Figures S4C–G), supporting the notion that immature neurons emerge in the hypothalamus following MSG treatment.

## Newly emerged AgRP neurons are not derived from *de novo* cell proliferation following MSG treatment

To evaluate whether the newly emerged AgRP neurons after MSG treatment are derived from *de novo* cell division, mice were given BrdU immediately following MSG or vehicle administration and were examined 7 days later. BrdU was administered twice daily via an intraperitoneal (i.p.) route for 3 days (Figure 4A) or in drinking water for 7 days (data not shown). Following MSG treatment, BrdU$^+$ cells were observed in the V-SVZ of the 3V corresponding to the location of α-tanycytes (Figure 4A). These BrdU$^+$ cells were often seen in doublets and co-expressed nestin (Figure 4B), suggesting that they are proliferating tanycytes. However, these BrdU$^+$ cells remained close to the V-SVZ and did not express a pan neuronal marker HuC/D or the *Npy*-GFP reporter in either vehicle- or MSG-treated mice (0 out of a total of 921 BrdU$^+$ cells quantified, VEH: 11.2 ± 4.0 and MSG: 35.7 ± 2.8 cells per 10 μm section, n=4–5 mice/group). To further investigate if BrdU$^+$ cells could differentiate into new neurons in the hypothalamus, we carried out a separate experiment in which a cohort of mice was given a single subcutaneous MSG injection and immediately provided with BrdU in drinking water for one week. Two weeks later, half of the mice received another injection of MSG (MSG+MSG group) with the remaining half receiving a vehicle administration (MSG+VEH group) (Figure 4C). These mice were sacrificed at 2

weeks after the last injection, allowing for a total chase duration of 4 weeks (Figure 4C). Most of the hypothalamic $BrdU^+$ cells in both the MSG+VEH and MSG+ MSG groups displayed a similar pattern, remaining close to the ventricular walls. Again, no BrdU expression was ever detected in $GFP^+$ AgRP neurons and we found no evidence of $BrdU^+$ neurons in neighboring hypothalamic parenchyma (0 out of a total of 1165 $BrdU^+$ cells quantified, MSG+VEH: 30.2 ± 2.5, MSG+MSG: 47.4 ± 1.1 cells per 10 μm section, n=6 mice/group). Thus, tanycytes proliferate in response to MSG-induced lesion, but despite their neurogenic potentials, proliferated tanycytes did not become AgRP neurons in the current experimental conditions. Instead, most of the proliferating tanycytes remain in the V-SVZ of the 3V. Collectively, these data indicated that the newly formed AgRP neurons following MSG treatment were not products of *de novo* cell division.

## Peripherally administered MSG ablates nearly all AgRP neurons in neonatal mice, a subset of which are replaced by cells derived from *Pomc*-expressing precursors

Compared with adult animals, MSG injection in neonatal rodents causes even more severe lesioning, as most ARC neurons are killed within 6 hours, and this is likely due to the incomplete formation of the BBB in the ARC of neonatal mice (Peruzzo et al., 2000). To investigate the extent of MSG-mediated ablation of AgRP neurons in neonatal mice, and to see if their numbers rebound as was seen in adult mice, 3-day-old (P3) *Npy*-GFP mice were subcutaneously injected with MSG, and their hypothalami were examined at P4, P11, and at both 4 and 13 weeks of life. A single injection of MSG in P3 mice eliminated almost all AgRP neurons within one day, and this was followed by the emergence of a small number of new AgRP neurons 7 days later (Figures 5A & 5C). These new AgRP neurons persisted for at least 4 weeks, but had disappeared by 13 weeks following MSG treatment (Figures 5A & 5C). AgRP immunoreactive fibers mirrored what was seen for ARC $GFP^+$ cell bodies after MSG insult (Figure 5B). These results suggest that both neonatal and adult mice possess the capacity to regenerate a small number of AgRP neurons that were ablated by MSG treatment and that, at least in neonatal mice, these newly formed neurons have a defined life-span. Consistent with what was seen in the adult mice, no $BrdU^+$ cell was found in AgRP neurons when assessed in neonatal mice 7 days after MSG and BrdU administration (data not shown).

The rapid nature of the post-ablative reconstitution of AgRP neurons in both adults and neonatal mice, together with the lack of BrdU incorporation in these newly emerged neurons, raises the possibility that they are derived from post-mitotic intermediate precursor cells. With this in mind, it is worth noting that half of the ARC *Pomc*-expressing cells generated during embryogenesis change their cell fate to become non-POMC cells such as AgRP and Kiss1 neurons (Padilla et al., 2010; Sanz et al., 2015). To explore the possibility that AgRP neurons emerging after MSG insult might be derived from descendants of *Pomc*-expressing cells, we performed a lineage tracing experiment in mice carrying *Tg.Pomc-Cre, Ai14(tdTomato), Npy-GFP* reporters, with the use of an independently generated *Tg.Pomc-Cre* line (Xu et al., 2005) that is distinct from the one used previously (Padilla et al., 2010). Using this strategy, $GFP^+$ cells within the ARC mark neurons that have a current AgRP identity, while tdTomato expression marks cells that are expressing POMC or have departed from their initial POMC identity to adopting a different cell fate. Thus, if AgRP neurons

were to be derived from *Pomc*-expressing precursor cells, these neurons can be identified by their co-expression of tdTomato and GFP (yellow cells). In unchallenged *Tg.Pomc-Cre, Ai14(tdTomato), Npy-GFP* mice, about 18.1% of *Npy*-GFP$^+$ AgRP neurons were also tdTomato$^+$ (Figure S5), consistent with the notion that some *Pomc*-expressing cells can adopt AgRP identity (Padilla et al., 2010).

The substantial number of AgRP neurons that escape MSG-mediated killing in adult mice prevents us to distinguish the newly emerged post-ablative AgRP neurons from those that survived MSG treatment in the first place. In contrast, MSG treatment in P3 neonatal mice achieved near complete elimination of all AgRP neurons (Figures 5A & 5C)(Broberger et al., 1998) allowing us to determine if any newly emerged AgRP neurons are derived from *Pomc*-expressing cells or their daughter cells. If none of the newly differentiated AgRP neurons originate from *Pomc*-expressing cells or their descendant cells, we would not expect to observe any cells co-expressing tdTomato and GFP. On the other hand, any double-positive cells seen among the newly emergent AgRP neurons would have been differentiated from cells with prior *Pomc* expression. Notably, when *Tg.Pomc-Cre, Ai14(tdTomato), Npy-GFP* mice were treated with MSG at P3 and evaluated at P11, some of the newly emerged cells were clearly doubly positive for tdTomato and GFP (1.8 ± 0.3 tdTomato$^+$ cells out of 13.1 ± 1.3 GFP$^+$ cells per section, n=5) (Figure 5D). These findings suggest that cells from the *Pomc*-expressing lineage are a source of post-mitotic precursors that can differentiate into AgRP neurons following MSG-induced lesioning.

## AgRP projections are most markedly reduced in the hindbrain of MSG-treated mice

We next investigated how AgRP fibers are affected by MSG treatment in adult mice. Three weeks post MSG or vehicle treatment, AgRP immunoreactive fibers were quantified in different regions of the brain, including bed nucleus of the stria terminalis (BNST), medial preoptic nucleus (MPO), paraventricular nucleus (PVN), paraventricular thalamic nucleus (PVT), dorsomedial hypothalamus (DMH), lateral hypothalamus (LHA), ARC, periaqueductal gray (PAG) and parabranchial nucleus (PBN). To avoid sampling bias due to position variability, serial sections spaced at 175 μm intervals from rostral to caudal regions of the brain were position-matched and quantified in a blinded fashion (Figure 6). Surprisingly, AgRP fiber density was not reduced to the same extent in rostral and caudal projection sites in that AgRP fiber density was more markedly reduced in the hindbrain regions (PAG and PBN) (Figure 6). The vulnerability of AgRP projections in the hindbrain regions to MSG-mediated ablation was reproduced in a different cohort of mice (data not shown).

Despite the severe lesioning of AgRP neurons, no gross phenotypic abnormality was observed in the days and weeks post-MSG treatment and MSG-treated mice maintained their body weight (Figures 7A–D). To examine if the animals retain the ability to mount a hyperphagic response after fasting, 8- to 9-week-old animals were placed in the Comprehensive Lab Animal Monitoring System (CLAMS). After baseline metabolic measurements were recorded, MSG or vehicle was administered. Food intake was transiently and slightly reduced on the day immediately following MSG injection, and it rebounded to control level in the second day, an observation that was reproduced in 3

different cohorts of animals. MSG-lesioned mice showed appropriate downregulation of energy expenditure upon fasting and exhibited normal hyperphagic refeeding. Respiratory exchange ratio (RER), motor activities, and fasting and refed glucose levels were similar between the two treatment groups (Figure 7). Thus, adult mice are able to cope with the profound loss of $AgRP^{OBBB}$ and maintain orexigenic drive.

## Discussion

The brain is protected by the BBB, a barrier along the vasculature consisting of endothelial tight junctions, astrocytic endfeet, pericytes and cellular basement membranes (Abbott et al., 2010). Tanycytes lining the ventral 3V are also important constituents of the BBB surrounding the ARC (Rodriguez et al., 2005). Many of the key metabolic hormones such as leptin and insulin are transported into the brain via special transport systems (Banks et al., 1996; Banks et al., 2012). For example, leptin is transported across the BBB via a saturable transport mechanism, but the amount of leptin transported into the brain is not proportional to the plasma leptin level due to the limited capacity of the transport machinery. This limited transport of leptin into the brain constitutes one of the mechanisms underlying leptin resistance, a hallmark of common obesity (Banks et al., 1999; Burguera et al., 2000). We previously showed that AgRP neurons are unique among hypothalamic neurons, as they are situated outside the BBB in the adult hypothalamus. $AgRP^{OBBB}$ are more sensitive to small changes in circulating leptin levels. They display dynamic SOCS3 expression after acute changes in dietary conditions, thereby acting as first-line responders to fine-tune metabolic responses (Olofsson et al., 2013). POMC neurons, another ARC neuronal cell type that act to oppose the actions of AgRP neurons, are primarily situated inside the BBB. POMC neurons, compared with AgRP neurons, exhibit delayed responses to leptin (Olofsson et al., 2013).

Although $AgRP^{OBBB}$ neurons have open communication with blood-borne metabolic signals, this study shows that they are also more vulnerable to circulating toxins. The preferential ablation of $AgRP^{OBBB}$ by MSG in adult animals highlights this vulnerability. The levels of MSG are normally high in the blood and its entry into the brain is prevented by the BBB (Hawkins, 2009). MSG is commonly used in the food industry as a favor enhancer. It has been documented that consumption of MSG is associated with increased weight gain in humans (He et al., 2011; He et al., 2008; Insawang et al., 2012), although some controversy surrounds this contention (Shi et al., 2010; Thu Hien et al., 2013). The dose of MSG used in this study (3.5 g/kg body weight, single dose) is about 35-fold higher than the highest amount of MSG consumed per day in adult humans (5.9–6 g per day) (He et al., 2011; Insawang et al., 2012), so it is unlikely that the amount of MSG consumed in adult humans is high enough to cause the death of $AgRP^{OBBB}$. However, chronic consumption of large amounts of MSG could potentially lead to excitation of $AgRP^{OBBB}$.

Our results indicate that the return of the AgRP neurons in adult mice after MSG insult is not due to *de novo* cell proliferation, as no BrdU was ever observed in AgRP neurons after 1 or 4 weeks of BrdU labeling. Our observation is in line with recent studies that α, but not β tanyctes, are self-renewing and neurospherogenic, but they rarely give rise to neurons in a non-stimulated hypothalamus (Robins et al., 2013). Instead, our results suggest that some of

the returning AgRP neurons, which make up about 28% of the lost neurons, can form rapidly after MSG-induced lesion from post-mitotic precursor cells. Currently, the identities of these post-mitotic precursors are not fully understood, but cells from the *Pomc*-expressing lineage may represent one source of these cells. Prior studies indicate that half of the embryonic *Pomc*-expressing precursors subsequently become non-POMC cells, some of which differentiate into AgRP/NPY neurons and Kiss1 neurons in the ARC (Padilla et al., 2010; Sanz et al., 2015). While the mechanism underlying neuronal transdifferentiation in the hypothalamus is currently not known, reprogramming of transcriptional machinery or microRNAs have been implicated to play important roles in trans-differentiation from non-neuronal cells to neurons (Shenoy and Blelloch, 2012; Tsunemoto et al., 2015). MicroRNAs also actively regulate expressions of hypothalamic neuropeptides and act as developmental switches (Messina et al., 2016).

In addition, tanycyte-derived cells could be another source of precursor cells. Lineage tracing experiment has shown that $Fgf10^{+}$ tanycytes can migrate and rapidly differentiate into neurons in the ARC within 8 days (Haan et al., 2013). It is interesting to note that $Fgf10^{+}$ tanycytes have proliferative capacity (Haan et al., 2013), so it is possible that a pool of post-mitotic cells from earlier cell divisions may reside in the adult hypothalamus, which can be induced to rapidly differentiate into neurons in response to lesioning. It is conceivable that the rates of stem cell proliferation into intermediate precursors and their terminal differentiation into neurons can be modulated by the abundance of the intermediate precursor pool and the age of the animals. In this regard, genetically-induced degeneration of AgRP neurons by mitochondrial deficiency, starting at early postnatal age, stimulates cell proliferation (Pierce and Xu, 2010). It is possible that under this setting, the early onset of AgRP neuronal degeneration in the postnatal brain and the progressive nature of the degeneration lead to constant usage of the intermediate precursor cell pool, which may subsequently stimulate cell division and rapid differentiation of these cells into neurons.

As a repair mechanism in response to acute and severe loss of $AgRP^{OBBB}$, trans-differentiation from post-mitotic intermediate precursor cells may provide faster metabolic relief, compared to *de novo* neurogenesis which normally takes several weeks to transition from cell proliferation to neuronal maturation (Lagace et al., 2007). The release of neuropeptides, in contrast to small neurotransmitters, does not require classical synapses (Ludwig and Leng, 2006; van den Pol, 2012). Thus, NPY and AgRP could be released from newly differentiated AgRP neurons and act on their target neurons within the ARC. These newly formed AgRP neurons could also generate local projections that inhibit neighboring POMC neurons. As $AgRP^{OBBB}$ act to fine-tune metabolic responses, an innate ability to replenish these neurons would ensure the functional integrity of these neuronal circuits. It is advantageous to possess a pool of intermediate precursor cells so that they can rapidly differentiate into neurons and provide immediate metabolic support. It is worth noting that the V-SVZ of the adult hypothalamus has abundant tanycytes that express neural stem cell markers such as GFAP and nestin, and they are highly proliferative in response to growth factor stimulation. Thus, *de novo* cell proliferation from neural stem cells may act over an extended period of time to replenish the drained intermediate precursor cell pool.

It should be noted that the extent of MSG-induced killing in the hypothalamus is much greater in the neonates than in the adult animals, and this is likely due to the incomplete formation of the BBB in the ARC of neonatal mice (Peruzzo et al., 2000). While the basic BBB in the brain is well-formed by birth (Abbott et al., 2010), astrocytes and tanycytes that comprise the BBB surrounding the ARC continue to develop in the postnatal weeks (Peruzzo et al., 2000; Rottkamp et al., 2015). It is noteworthy that MSG treatment in neonatal animals leads to development of obesity later in life. The maturation of rodent brain between postnatal days P1 to P10 corresponds approximately to that in the 3rd trimester of human gestation (Clancy et al., 2007). This postnatal week marks a critical period in hypothalamic development as many of the hypothalamic neurons adopt their permanent cell fate, establish connectivity with other neurons, and become responsive to peripheral metabolic hormones (Bouret et al., 2004; Padilla et al., 2010; Rottkamp et al., 2015; Sanz et al., 2015). MSG administration in neonatal mice ablates almost all AgRP neurons ((Broberger et al., 1998) and this study). Although MSG may damage anorexigenic neurons, it is worth noting that selective ablation of the entire population of neonatal AgRP neurons by diphtheria toxin leads to obesity later in life (Joly-Amado et al., 2012). Thus, the neonatal hypothalamus has tremendous plasticity and can readily adapt to the loss of all AgRP neurons via development of compensatory mechanisms. In direct contrast to neonatal mice, acute ablation of all AgRP neurons in adult mice leads to severe anorexia and weight loss (Luquet et al., 2005). This suggests that AgRP neurons are indispensable for life and that the adult hypothalamus has lost the ability to cope with the acute loss of all AgRP neurons. Remarkably, ablation of $AgRP^{OBBB}$ by MSG in adult neurons does not produce alteration of feeding and body weight. One possibility is that intact AgRP neurons behind the BBB along with newly formed neurons are able to provide sufficient orexigenic drive. Another possibility is that $AgRP^{OBBB}$ sensitive to MSG may only affect a subset of AgRP neuronal functions. It is interesting to note that AgRP axonal projections targeting different brain regions originate from distinct AgRP neuronal subpopulations (Betley et al., 2013). While AgRP neuronal subpopulations that project to the anterior BNST, PVH, LHA, or PVT are sufficient to evoke acute feeding, those that target the CEA, PAG, and PBN are not (Betley et al., 2013). Our observation that AgRP fibers in the hindbrain area (PAG and PBN) are more dramatically affected by MSG raises the possibility that $AgRP^{OBBB}$ may play important roles in regulating neuronal functions in the hindbrain. It should be noted that substantial AgRP fibers remain in the hindbrain of MSG-treated mice following ablation (an average of 50.2% in PAG and 29.4% in PBN), suggesting that some AgRP neurons inside the BBB also project to the hindbrain. We should emphasize that the current method of quantifying fiber density may not have the sensitivity to detect small differences. While our data indicate that $AgRP^{OBBB}$ project to the hindbrain, current methodology does not rule out that this specific population of neurons may also project to other forebrain regions. New strategies will need to be developed to direct gene expression specifically in $AgRP^{OBBB}$ so that their functions, projections and downstream neuronal targets can be further determined.

While MSG-induced ablation of $AgRP^{OBBB}$ represents an extreme scenario, subdued “wear and tear” of a small number of AgRP neurons could occur more frequently under physiological or pathological settings such as obesity, diabetes or substance abuse, as these neurons are directly exposed to circulating molecules that could be neurotoxic. Thus,

although metabolically less adaptable compared to neonates, adult animals still possess remarkable ability to cope with the lesioning of neurons outside the BBB, as the acute loss of $AgRP^{OBBB}$ produces very little short-term metabolic consequences in adult mice. While the rapid formation of AgRP neurons after MSG-induced lesioning may help sustain orexigenic drive, it also buys time so that additional compensatory mechanisms can be developed. Our results show that MSG treatment in neonates leads to ablation of all AgRP neurons, and that the newly returned AgRP neurons have a finite lifespan. This observation suggests that AgRP neurons are no longer needed in adult animals once compensatory mechanisms have developed in the MSG-treated neonatal mice. In support of this notion, adult mice can ultimately tolerate diphtheria toxin-mediated ablation of all AgRP neurons if energy supply can be sustained for a period of time by forced feeding or via ample adipose tissue reserve (Wu et al., 2012). These studies indicate that once these compensatory mechanisms are developed, AgRP neurons become dispensable.

In summary, our study suggests that multiple mechanisms may operate in concert to allow animals to cope with the acute loss of $AgRP^{OBBB}$. First, despite the majority of orexigenic AgRP neurons being outside the BBB, a substantial number of AgRP neurons are protected by the BBB. Second, the rapid differentiation of AgRP neurons from intermediate precursor cells could provide immediate metabolic relief as discussed above. Third, proliferation of tanycytes is robustly stimulated upon MSG-induced lesioning, and these newly proliferated cells may act to replenish the intermediate precursor cell pool. In addition to acting as neural precursor cells, tanycytes are also important for communication between cerebrospinal fluid (CSF) and hypothalamic portal capillaries, and transport of macromolecules such as glucose, glutamate, and leptin (Balland et al., 2014; Bolborea and Dale, 2013; Peruzzo et al., 2000; Rodriguez et al., 2005). Tanycytes also participate in the regulation of BBB permeability as structural organization of the blood-to-hypothalamus barrier is modulated by fasting (Langlet et al., 2013). Thus, proliferation of tanycytes after MSG-mediated lesioning may represent an important adaptive mechanism. Taken together, all of these mechanisms may act in concert to ensure proper metabolic control in response to acute loss of a large number of orexigenic neurons.

## Experimental Procedures

### Mice

All animal care and experiments were approved by the University of California at San Francisco Institutional Animal Care and Use Committee. All experiments were performed using male mice, except where noted. Mice were group-housed (12 hr light/dark) and age matched. Mice were fed a standard mouse chow (21.6% from fat; Purina mouse diet #5058). *Npy*-GFP mice [B6.FVB-Tg(*Npy*-hrGFP)1Lowl/J] and *Ai14(tdTomato)* mice [B6;129S6-*Gt(ROSA)26Sor*$^{tm14(CAG\text{-}tdTomato)Hze}$/J] were purchased from Jackson Laboratory. *AgRP-CreER*$^{T2}$ mice were kindly provided by Dr. Joel Elmquist (UT Southwestern, Texas). The *Tg.PomcCre* and *AgRP-CreER*$^{T2}$ lines were maintained as heterozygotes on C57Bl/6 background.

### bFGF infusion

Osmotic minipumps (model 1007D flow rate 0.5 μl/h, 7 days, Alzet, Durec Inc) containing 3.2 mg/ml BrdU or BrdU and 100 μg/ml bFGF solution were connected to steel guide cannula (Alzet) implanted into the right lateral ventricle. Surgical procedures and solution preparation are detailed in Supplemental Experimental Procedures.

### BrdU

For i.p. administration, a 10 mg/ml BrdU solution was administered twice-daily (8 hours apart) at a dose of 0.1 g/kg. To administer BrdU via drinking water, mice were placed in cages in which the only source of water contained 1 mg/ml of BrdU and 0.25 mg/ml of glucose (to alleviate aversion to the possible bitter taste of BrdU). The solution was replaced every 2 days with freshly prepared solution. For i.c.v. delivery, osmotic minipumps were prefilled with 1 mg/ml solution of BrdU in artificial CSF and delivered via a steel guide cannula into the lateral ventricle. Surgical procedures are described in Supplemental Experimental Procedures.

### Ablation of cells outside the BBB

Mice received subcutaneous injection of MSG at a dose of 3.5 g/kg or isomolar sodium chloride solution as vehicle (0.02 M/kg, or 1.2 g/kg). All solutions were prepared on the day of injection and filter-sterilized. All mice received one dose of MSG or vehicle except where noted.

### Evaluation of BBB by Evans Blue

To mark AgRP$^{OBBB}$, *Npy*-GFP mice were anesthetized and injected transcardially with 50 μl Evans Blue solution (1% w/v in saline) (Sigma). Mice were subsequently perfused with 4% (w/v) paraformaldehyde (PFA) 10 min later. Direct fluorescence emitted by Evans Blue was captured from cryosections immediately following coverslipping.

### Tamoxifen administration

Tamoxifen (Tx)(Sigma) was prepared in corn oil and filter-sterilized. AgRP-CreER$^{T2}$ mice were fasted at the onset of dark phase and were injected subcutaneously with 400 mg/kg of tamoxifen 18 hours later. Free access to food was allowed after 24 hours of fasting.

### Immunofluorescence

Anesthesized mice were perfused with 4% (w/v) PFA. Brains were postfixed in 4% PFA, and immersed in 30% sucrose overnight and sectioned at 10 μm on a cryostat, except Figures 3A, 3C & 7, where 35-μm sections were used. Immunohistochemistry was performed using the following antibodies: goat anti AgRP (1:1000, Neuromics), rabbit anti DCX (1:500, Abcam), rat anti BrdU (1:200, AbD serotec), mouse anti NeuN (1:200, Chemicon), mouse anti HuC/D (1:2000, Invitrogen) and mouse anti nestin (1:200, Millipore). For staining of DCX, HuC/D, and NeuN, sections were subjected to heat-mediated antigen retrieval in a 10 mM citrate solution. For BrdU staining, sections were incubated in a 1N hydrochloric acid solution at 55°C for 3 minutes. Sections were incubated in a blocking solution followed by primary antibody overnight at 4°C and washed. A

solution of secondary antibodies was then applied for 1 hour at room temperature. Images were acquired with an Olympus BX51WI microscope equipped with a QImaging Retiga 2000R digital camera. Double-immunofluorescence analyses of BrdU and NeuN, HuC/D or nestin were done by applying the two different antibodies sequentially. Pictures taken before and after immunohistochemistry were merged in Adobe Photoshop software using anatomical landmarks.

### Cell Counting

Neuronal quantification was performed using ImageJ software in matched sections containing the ARC (Bregma −1.94 to −2.30 mm). For quantification of cells in the mediobasal and lateral ARC, the arcuate nucleus was identified by neuroanatomical landmark and divided into 3 quadrants along the 3V. Two ventral quadrants encompassing the median eminence are taken as the mediobasal partition which represents area outside of the BBB as marked by Evans Blue uptake, and the upper quadrant is taken as the lateral partition and represents area inside the BBB. More details on cell counting are provided in Supplemental Experimental Procedures.

### Neurite quantification

AgRP neurite quantification was performed in matched (Supplemental Experimental Procedures) 35-μm-thick serial sections distanced at 175 μm apart. Sections were blinded prior to analyses using imageJ software. For image analysis, briefly, threshold was applied for each image such that labeled fibers were isolated from the background in a binary fashion. In the binarized image, the presence of AgRP neurites was calculated as an area which reflects the total number of pixels positive for AgRP signal. AgRP neurites in distinct nuclei were quantified over a selected area encompassing the region based on neuroanatomical landmarks.

### Metabolic studies

Animals were single-housed 3 days before food intake, calculated as the weight of food taken from the hopper, was measured. Body weight was recorded daily at 10 AM. For fasting-induced feeding measurements, mice were transferred to a new cage with fresh bedding without food at 10 AM. Food was provided 24 hours after the commencement of fasting and food intake was measured for the next 24 hours. Blood glucose measurements were taken using the FreeStyle Lite glucometer (Abbott). For metabolic monitoring, mice were single-housed for 3 days prior to commencement of measurement and allowed one day to acclimatize in CLAMS chambers. $O_2$ consumption, $CO_2$ production, food intake, and locomotor activities were analysed by CLAMS. All experiment was performed in room temperature except for Figures 7C & 7E–7L where mice were maintained at thermoneutral condition of 30°C.

### Statistics

All data are expressed as mean ± SEM. A two-tailed Student’s t test was used to test the difference between two groups of mice. In cases where multiple independent groups were compared, one-way ANOVA followed by post-hoc test were performed. In cases where the

same animals were analyzed over time, two-way repeated measures ANOVA was used followed by a multiple comparison analysis. Statistical analyses were assessed using Prism software (Graphpad Software, Inc.). Differences were regarded as statistically significant if $P<0.05$.

## Supplementary Material

Refer to Web version on PubMed Central for supplementary material.

## Acknowledgments

We thank Dr. Joel Elmquist at UT-Southwestern University for providing the *Agrp-CreER*$^{T2}$ mice. This study was supported by NIH NIDDK1R01DK089094-01 to AWX and in part by the Kraft Fellowship in Stem Cell Research to EY. The work is also partly supported by the Mouse Metabolism Core at the UCSF Nutrition Obesity Center (NIH NIDDK 1P30DK098722-01A1), and the Microscopy Core at the UCSF Diabetes Endocrinology Research Center (NIH NIDDK P30 DK63720-06A1).

## References

Abbott NJ, Patabendige AA, Dolman DE, Yusof SR, Begley DJ. Structure and function of the blood-brain barrier. Neurobiol Dis. 2010; 37:13–25. [PubMed: 19664713]

Abraham R, Dougherty W, Golberg L, Coulston F. The response of the hypothalamus to high doses of monosodium glutamate in mice and monkeys. Cytochemistry and ultrastructural study of lysosomal changes. Exp Mol Pathol. 1971; 15:43–60. [PubMed: 4998013]

Aponte Y, Atasoy D, Sternson SM. AGRP neurons are sufficient to orchestrate feeding behavior rapidly and without training. Nat Neurosci. 2011; 14:351–355. [PubMed: 21209617]

Balland E, Dam J, Langlet F, Caron E, Steculorum S, Messina A, Rasika S, Falluel-Morel A, Anouar Y, Dehouck B, et al. Hypothalamic tanycytes are an ERK-gated conduit for leptin into the brain. Cell Metab. 2014; 19:293–301. [PubMed: 24506870]

Banks WA, DiPalma CR, Farrell CL. Impaired transport of leptin across the blood-brain barrier in obesity. Peptides. 1999; 20:1341–1345. [PubMed: 10612449]

Banks WA, Kastin AJ, Huang W, Jaspan JB, Maness LM. Leptin enters the brain by a saturable system independent of insulin. Peptides. 1996; 17:305–311. [PubMed: 8801538]

Banks WA, Owen JB, Erickson MA. Insulin in the brain: there and back again. Pharmacol Ther. 2012; 136:82–93. [PubMed: 22820012]

Betley JN, Cao ZF, Ritola KD, Sternson SM. Parallel, redundant circuit organization for homeostatic control of feeding behavior. Cell. 2013; 155:1337–1350. [PubMed: 24315102]

Bolborea M, Dale N. Hypothalamic tanycytes: potential roles in the control of feeding and energy balance. Trends Neurosci. 2013; 36:91–100. [PubMed: 23332797]

Bouret SG, Draper SJ, Simerly RB. Trophic action of leptin on hypothalamic neurons that regulate feeding. Science. 2004; 304:108–110. [PubMed: 15064420]

Broberger C, Johansen J, Johansson C, Schalling M, Hokfelt T. The neuropeptide Y/agouti gene-related protein (AGRP) brain circuitry in normal, anorectic, and monosodium glutamate-treated mice. Proc Natl Acad Sci U S A. 1998; 95:15043–15048. [PubMed: 9844012]

Burde RM, Schainker B, Kayes J. Acute effect of oral and subcutaneous administration of monosodium glutamate on the arcuate nucleus of the hypothalamus in mice and rats. Nature. 1971; 233:58–60. [PubMed: 12058742]

Burguera B, Couce ME, Curran GL, Jensen MD, Lloyd RV, Cleary MP, Poduslo JF. Obesity is associated with a decreased leptin transport across the blood-brain barrier in rats. Diabetes. 2000; 49:1219–1223. [PubMed: 10909981]

Clancy B, Finlay BL, Darlington RB, Anand KJ. Extrapolating brain development from experimental species to humans. Neurotoxicology. 2007; 28:931–937. [PubMed: 17368774]

Haan N, Goodman T, Najdi-Samiei A, Stratford CM, Rice R, El Agha E, Bellusci S, Hajihosseini MK. Fgf10-expressing tanycytes add new neurons to the appetite/energy-balance regulating centers of the postnatal and adult hypothalamus. J Neurosci. 2013; 33:6170–6180. [PubMed: 23554498]

Hawkins RA. The blood-brain barrier and glutamate. Am J Clin Nutr. 2009; 90:867S–874S. [PubMed: 19571220]

He K, Du S, Xun P, Sharma S, Wang H, Zhai F, Popkin B. Consumption of monosodium glutamate in relation to incidence of overweight in Chinese adults: China Health and Nutrition Survey (CHNS). Am J Clin Nutr. 2011; 93:1328–1336. [PubMed: 21471280]

He K, Zhao L, Daviglus ML, Dyer AR, Van Horn L, Garside D, Zhu L, Guo D, Wu Y, Zhou B, et al. Association of monosodium glutamate intake with overweight in Chinese adults: the INTERMAP Study. Obesity (Silver Spring). 2008; 16:1875–1880. [PubMed: 18497735]

Insawang T, Selmi C, Cha'on U, Pethlert S, Yongvanit P, Areejitranusorn P, Boonsiri P, Khampitak T, Tangrassameeprasert R, Pinitsoontorn C, et al. Monosodium glutamate (MSG) intake is associated with the prevalence of metabolic syndrome in a rural Thai population. Nutr Metab (Lond). 2012; 9:50. [PubMed: 22681873]

Ishii Y, Bouret SG. Embryonic birthdate of hypothalamic leptin-activated neurons in mice. Endocrinology. 2012; 153:3657–3667. [PubMed: 22621961]

Joly-Amado A, Denis RG, Castel J, Lacombe A, Cansell C, Rouch C, Kassis N, Dairou J, Cani PD, Ventura-Clapier R, et al. Hypothalamic AgRP-neurons control peripheral substrate utilization and nutrient partitioning. Embo J. 2012; 31:4276–4288. [PubMed: 22990237]

Kokoeva MV, Yin H, Flier JS. Evidence for constitutive neural cell proliferation in the adult murine hypothalamus. J Comp Neurol. 2007; 505:209–220. [PubMed: 17853440]

Krashes MJ, Koda S, Ye C, Rogan SC, Adams AC, Cusher DS, Maratos-Flier E, Roth BL, Lowell BB. Rapid, reversible activation of AgRP neurons drives feeding behavior in mice. J Clin Invest. 2011; 121:1424–1428. [PubMed: 21364278]

Kriegstein A, Alvarez-Buylla A. The glial nature of embryonic and adult neural stem cells. Annu Rev Neurosci. 2009; 32:149–184. [PubMed: 19555289]

Lagace DC, Whitman MC, Noonan MA, Ables JL, DeCarolis NA, Arguello AA, Donovan MH, Fischer SJ, Farnbauch LA, Beech RD, et al. Dynamic contribution of nestin-expressing stem cells to adult neurogenesis. J Neurosci. 2007; 27:12623–12629. [PubMed: 18003841]

Langlet F, Levin BE, Luquet S, Mazzone M, Messina A, Dunn-Meynell AA, Balland E, Lacombe A, Mazur D, Carmeliet P, et al. Tanycytic VEGF-A boosts blood-hypothalamus barrier plasticity and access of metabolic signals to the arcuate nucleus in response to fasting. Cell Metab. 2013; 17:607–617. [PubMed: 23562080]

Ludwig M, Leng G. Dendritic peptide release and peptide-dependent behaviours. Nat Rev Neurosci. 2006; 7:126–136. [PubMed: 16429122]

Luquet S, Perez FA, Hnasko TS, Palmiter RD. NPY/AgRP neurons are essential for feeding in adult mice but can be ablated in neonates. Science. 2005; 310:683–685. [PubMed: 16254186]

Markakis EA, Palmer TD, Randolph-Moore L, Rakic P, Gage FH. Novel neuronal phenotypes from neural progenitor cells. J Neurosci. 2004; 24:2886–2897. [PubMed: 15044527]

McNay DE, Briancon N, Kokoeva MV, Maratos-Flier E, Flier JS. Remodeling of the arcuate nucleus energy-balance circuit is inhibited in obese mice. J Clin Invest. 2012; 122:142–152. [PubMed: 22201680]

Messina A, Langlet F, Chachlaki K, Roa J, Rasika S, Jouy N, Gallet S, Gaytan F, Parkash J, Tena-Sempere M, et al. A microRNA switch regulates the rise in hypothalamic GnRH production before puberty. Nat Neurosci. 2016; 19:835–844. [PubMed: 27135215]

Olney JW. Brain lesions, obesity, and other disturbances in mice treated with monosodium glutamate. Science. 1969; 164:719–721. [PubMed: 5778021]

Olney JW, Sharpe LG. Brain lesions in an infant rhesus monkey treated with monsodium glutamate. Science. 1969; 166:386–388. [PubMed: 5812037]

Olofsson LE, Unger EK, Cheung CC, Xu AW. Modulation of AgRP-neuronal function by SOCS3 as an initiating event in diet-induced hypothalamic leptin resistance. Proc Natl Acad Sci U S A. 2013; 110:E697–706. [PubMed: 23386726]

Padilla SL, Carmody JS, Zeltser LM. Pomc-expressing progenitors give rise to antagonistic neuronal populations in hypothalamic feeding circuits. Nat Med. 2010; 16:403–405. [PubMed: 20348924]

Peruzzo B, Pastor FE, Blazquez JL, Schobitz K, Pelaez B, Amat P, Rodriguez EM. A second look at the barriers of the medial basal hypothalamus. Exp Brain Res. 2000; 132:10–26. [PubMed: 10836632]

Pierce AA, Xu AW. De novo neurogenesis in adult hypothalamus as a compensatory mechanism to regulate energy balance. J Neurosci. 2010; 30:723–730. [PubMed: 20071537]

Robins SC, Stewart I, McNay DE, Taylor V, Giachino C, Goetz M, Ninkovic J, Briancon N, Maratos-Flier E, Flier JS, et al. alpha-Tanycytes of the adult hypothalamic third ventricle include distinct populations of FGF-responsive neural progenitors. Nat Commun. 2013; 4:2049. [PubMed: 23804023]

Rodriguez EM, Blazquez JL, Pastor FE, Pelaez B, Pena P, Peruzzo B, Amat P. Hypothalamic tanycytes: a key component of brain-endocrine interaction. Int Rev Cytol. 2005; 247:89–164. [PubMed: 16344112]

Rottkamp DM, Rudenko IA, Maier MT, Roshanbin S, Yulyaningsih E, Perez L, Valdearcos M, Chua S, Koliwad SK, Xu AW. Leptin potentiates astrogenesis in the developing hypothalamus. Mol Metab. 2015; 4:881–889. [PubMed: 26629411]

Sanz E, Quintana A, Deem JD, Steiner RA, Palmiter RD, McKnight GS. Fertility-regulating Kiss1 neurons arise from hypothalamic POMC-expressing progenitors. J Neurosci. 2015; 35:5549–5556. [PubMed: 25855171]

Shenoy A, Blelloch R. microRNA induced transdifferentiation. F1000 Biol Rep. 2012; 4:3. [PubMed: 22312415]

Shi Z, Luscombe-Marsh ND, Wittert GA, Yuan B, Dai Y, Pan X, Taylor AW. Monosodium glutamate is not associated with obesity or a greater prevalence of weight gain over 5 years: findings from the Jiangsu Nutrition Study of Chinese adults. Br J Nutr. 2010; 104:457–463. [PubMed: 20370941]

Thu Hien VT, Thi Lam N, Cong Khan N, Wakita A, Yamamoto S. Monosodium glutamate is not associated with overweight in Vietnamese adults. Public Health Nutr. 2013; 16:922–927. [PubMed: 22894833]

Tsunemoto RK, Eade KT, Blanchard JW, Baldwin KK. Forward engineering neuronal diversity using direct reprogramming. EMBO J. 2015; 34:1445–1455. [PubMed: 25908841]

van den Pol AN. Neuropeptide transmission in brain circuits. Neuron. 2012; 76:98–115. [PubMed: 23040809]

Wang Q, Liu C, Uchida A, Chuang JC, Walker A, Liu T, Osborne-Lawrence S, Mason BL, Mosher C, Berglund ED, et al. Arcuate AgRP neurons mediate orexigenic and glucoregulatory actions of ghrelin. Mol Metab. 2014; 3:64–72. [PubMed: 24567905]

Werner L, Muller-Fielitz H, Ritzal M, Werner T, Rossner M, Schwaninger M. Involvement of doublecortin-expressing cells in the arcuate nucleus in body weight regulation. Endocrinology. 2012; 153:2655–2664. [PubMed: 22492306]

Wu Q, Whiddon BB, Palmiter RD. Ablation of neurons expressing agouti-related protein, but not melanin concentrating hormone, in leptin-deficient mice restores metabolic functions and fertility. Proc Natl Acad Sci U S A. 2012; 109:3155–3160. [PubMed: 22232663]

Xu AW, Kaelin CB, Takeda K, Akira S, Schwartz MW, Barsh GS. PI3K integrates the action of insulin and leptin on hypothalamic neurons. J Clin Invest. 2005; 115:951–958. [PubMed: 15761497]

Ye R, Wang QA, Tao C, Vishvanath L, Shao M, McDonald JG, Gupta RK, Scherer PE. Impact of tamoxifen on adipocyte lineage tracing: Inducer of adipogenesis and prolonged nuclear translocation of Cre recombinase. Mol Metab. 2015; 4:771–778. [PubMed: 26629402]

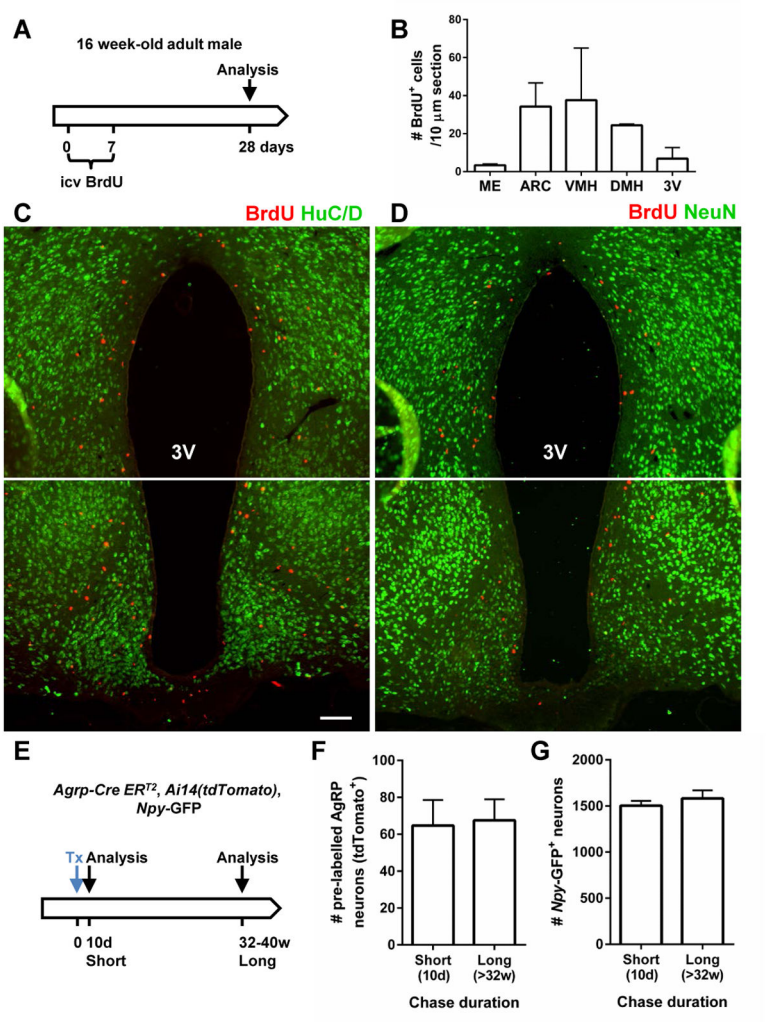


**Figure 1. Lack of *de novo* neurogenesis and absence of basal turnover of AgRP neurons in normal adult animals**

(**A–D**) Schematic representation of experiment (Panel **A**): 16-week-old mice received i. c. v. infusion of BrdU for 7 days and were sacrificed 28 days later. Hypothalamic sections were immunostained with BrdU (red) and HuC/D (green, Panel **C**) or NeuN (green, Panel **D**) antibodies. HuC/D$^+$ and NeuN$^+$ cells do not incorporate BrdU. 3V: 3$^{rd}$ ventricle. Scale bar: 100 µm. **B**. Quantification of BrdU$^+$ cells in the ME, ARC, VMH, DMH and the wall of the 3V (n=2/group). Data are means ± SEM. (**E–G**) Schematic representation of experiment (Panel **E**): adult male *Agrp-CreER$^{T2}$* mice carrying the *Npy*-GFP and tdTomato reporters received administration of Tx to induce the expression of tdTomato in AgRP neurons. Mice were sacrificed following a short (10 days) or long chase (32–40 weeks). (**F**) Quantification of the number of tdTomato$^+$/GFP$^+$ and (**G**) GFP$^+$ cells in the ARC following the short- or long-term chase duration (n=7/group). Data are means ± SEM.

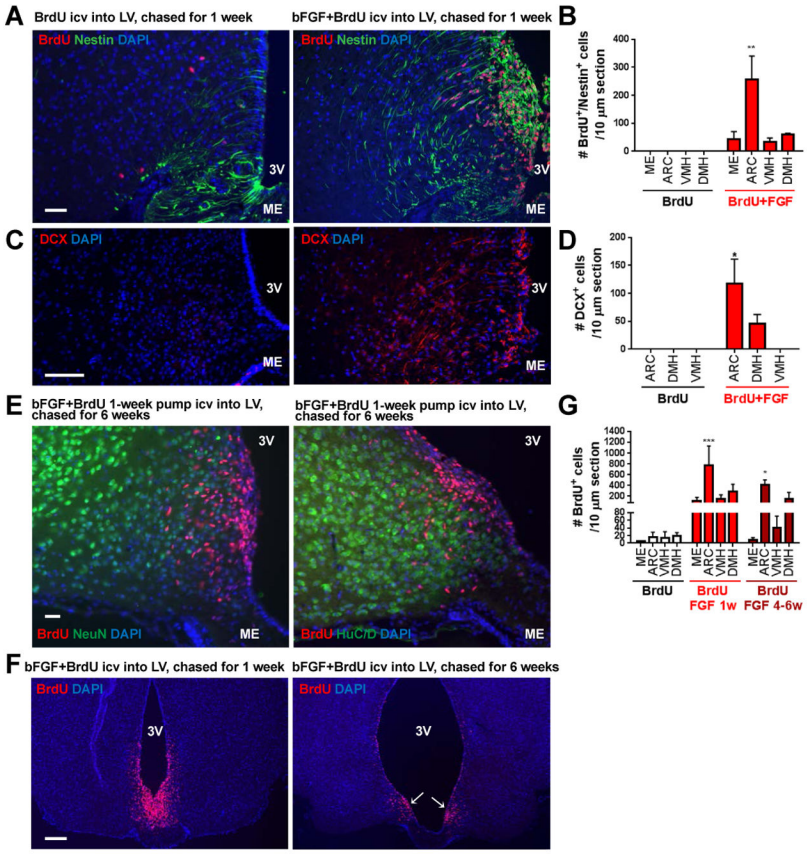


**Figure 2. bFGF stimulates proliferation of tanycytes, but they do not become neurons under normal conditions**

(**A**) Relative to vehicle-treatment, i.c.v. infusion of bFGF for 1 week led to a dramatic increase in nestin expression (green) and incorporation of BrdU (red) in the V-SVZ of the 3V. Scale bar: 50 µm. (**B**) Quantification of $BrdU^+$/$nestin^+$ cells in FGF-infused and control mice. No $BrdU^+$/$nestin^+$ cells were detected in vehicle mice. (**C**) Infusion of bFGF for 1 week led to an increase in DCX expression (red), a marker for immature neurons. Scale bar: 50 µm. (**D**) Quantification of $DCX^+$ cells in FGF-infused and control mice. No $DCX^+$ cells were detected in vehicle mice. (**E**) Despite abundant $BrdU^+$ cells being observed in the hypothalamus, no $BrdU^+$ cells were found to co-express neuronal marker NeuN (left panel) or HuC/D (right panel). Scale bar: 50 µm. (**F**) After i.c.v. infusion of bFGF for 1 week (left panel), most $BrdU^+$ cells were found in the V-SVZ of the ventral 3V. Six weeks after bFGF infusion into the lateral ventricle, most of the $BrdU^+$ cells remained in the V-SVZ where α-tanycytes are located (arrows, right panel), as well as in adjacent ARC parenchyma. Scale bar: 200 µm. (**G**) Quantification of $BrdU^+$ cells in mice sacrificed after 1 or 4–6 weeks after BrdU+FGF infusion relative to controls. Data are means ± SEM of n=2/group.* P<0.05, ** P<0.01, *** P<0.001 as determined by two-way repeated measures ANOVA, followed by Sidak's multiple comparisons tests for the discrete brain regions examined. 3V: 3rd ventricle, ME: median eminence. DCX: doublecortin.

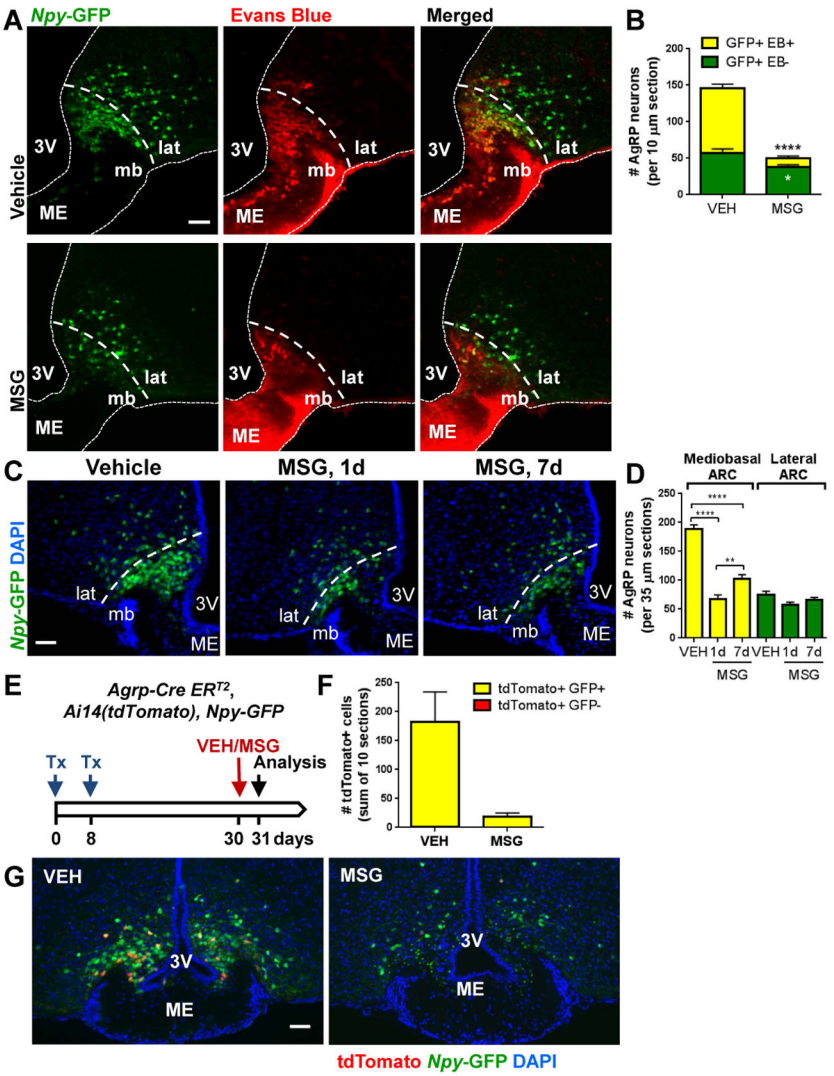


**Figure 3. Peripheral administration of MSG in adult mice rapidly ablates AgRP$^{OBBB}$, followed by rapid emergence of a small number of newly differentiated AgRP neurons**

(**A**) Representative sections from vehicle- and MSG-treated adult mice show that AgRP neurons (green) in the mediobasal, but not those in the lateral ARC incorporate peripherally-infused Evans Blue (red) and are preferentially ablated by MSG. (**B**) Quantification of Evans Blue$^{+}$ and Evans Blue$^{-}$ AgRP neurons 1 day following MSG administration in adult female mice (n=7–8/group). Data are means ± SEM, * P<0.05, **** P<0.0001 compared to the corresponding vehicle value as determined by unpaired t tests. (**C**) Representative sections showing the number of AgRP neurons in the mediobasal and lateral ARC in adult *Npy*-GFP mice following vehicle or MSG treatment. (**D**) Quantification of AgRP neurons in the mediobasal and lateral ARC (n= 5–10/group). Data are means ± SEM, ** p ≤ 0.01, **** p ≤ 0.0001 as determined by one-way ANOVA, followed by Dunnett's multiple comparison tests. (**E–G**): adult *Agrp-CreER$^{T2}$* mice carrying the *Npy*-GFP and tdTomato reporters received 2 Tx injections at 1 week apart to induce the expression of tdTomato in AgRP neurons. Vehicle or MSG was administered 30 days later and mice were sacrifice at the following day. (**F**) Quantification of AgRP neurons expressing tdTomato (red) or tdTomato

and GFP reporters (yellow) in the ARC (n=3/group). No tdTomato$^{+}$/Npy-GFP$^{-}$ neurons were detected in brains analyzed 1 day after MSG administration. Data are means ± SEM. (**G**) Representative sections showing expression of tdTomato (red) in a subset of AgRP neurons (green) in vehicle- and MSG-treated animals. 3V: 3$^{rd}$ ventricle, ME: median eminence, mb: mediobasal, lat: lateral. Scale bars: 50 μm.

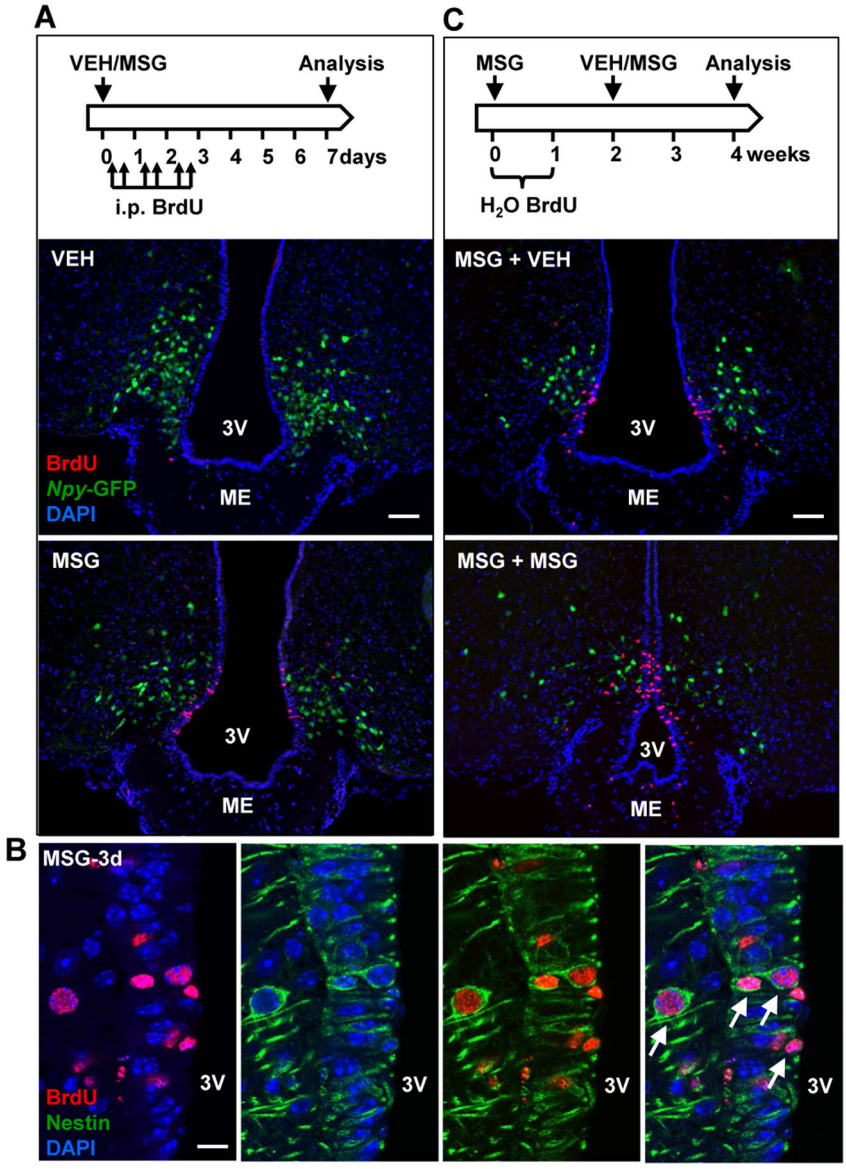


**Figure 4. Newly emergent AgRP neurons are not derived from cells that proliferated after MSG-induced insult**

(**A**) Vehicle or MSG was administered to 8-week-old mice carrying the *Npy*-GFP reporter, following which BrdU was administered i.p. twice daily for 3 days. Mice were sacrificed at day 7. Compared to vehicle controls, MSG-treated mice showed increased BrdU (red) incorporation in the V-SVZ of the 3V corresponding to the location of α-tanycytes. No $BrdU^+$ AgRP neurons (green) were detected. Scale bar: 50 μm. (**B**) Following MSG administration, mice received twice daily i.p. BrdU injections until they were sacrificed 3 days later. Representative single optical scan confocal microscopy shows $BrdU^+$/$nestin^+$ cells (arrows) in the V-SVZ of the 3V. Scale bar: 10 μm. (**C**) 6-week-old *Npy*-GFP mice received MSG administration and were given BrdU in drinking water for 1 week. Following the initial MSG treatment, mice received an additional vehicle (MSG+VEH) or MSG administration (MSG+MSG) at 2 weeks and were sacrificed at 4 weeks. Representative

sections from mice receiving MSG+VEH and MSG+MSG show that $BrdU^+$ cells (red) do not express the *Npy*-GFP reporter (green). Scale bar: 50 μm. ME: median eminence, 3V: 3rd ventricle.

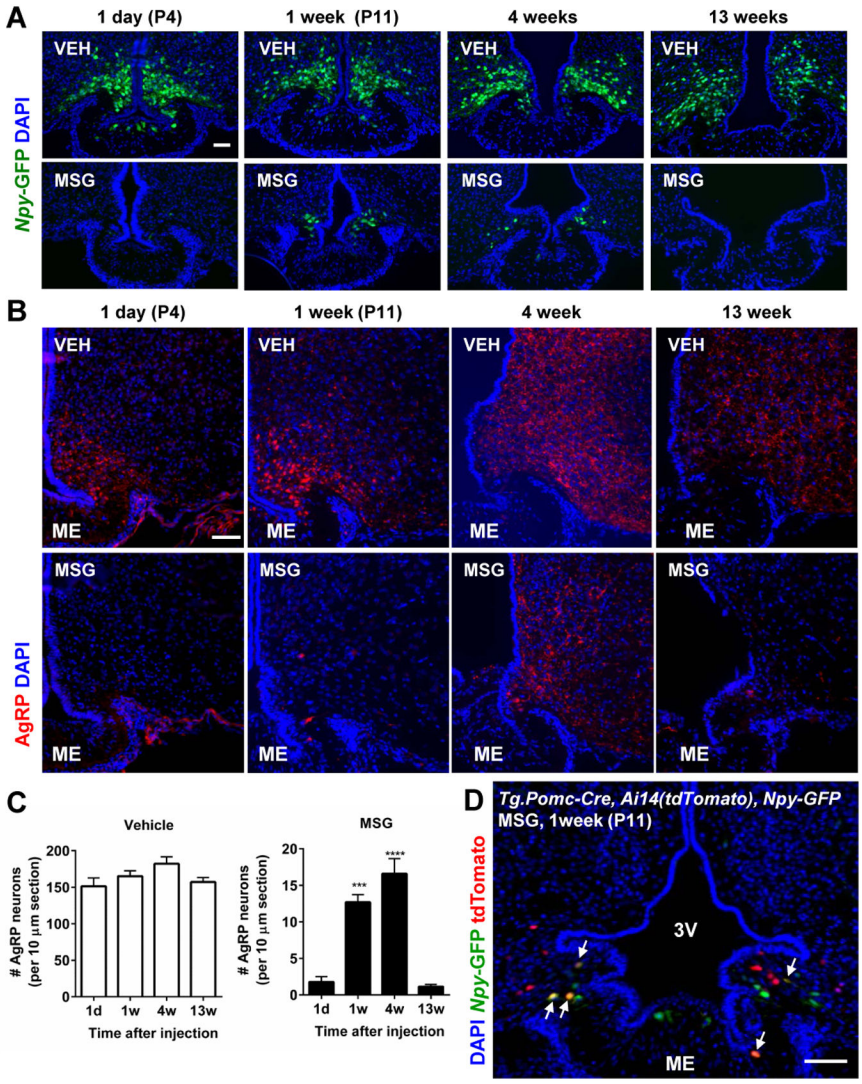


**Figure 5. A subset of newly emergent AgRP neurons are derived from *Pomc*-expressing precursor cells in neonatal mice**

Male and female neonatal pups were given an injection of vehicle or MSG at postnatal day 3 (P3) and were examined at 1 day (P4), 1 week (P11), 4 weeks, or 13 weeks later. (**A–B**) Representative sections showing the number of AgRP neurons (green) (**A**) and AgRP immunoreactive fibers (red fibers) (**B**) in vehicle- or MSG-treated mice at the various time points post-treatment. (**C**) Quantification of the number of AgRP neurons in *Npy*-GFP mice at 1 day, 1 week, 4 weeks or 13 weeks following vehicle or MSG treatment at postnatal day 3 (n=3–8/group). Data are means ± SEM, *** $p \leq 0.001$, **** $p \leq 0.0001$ versus 1 day after vehicle or MSG as determined by one-way ANOVA, followed by Dunnett's multiple comparison test. (**D**) *Tg.Pomc-Cre, Ai14(tdTomato), Npy*-GFP mice received an administration of MSG at postnatal day 3 (P3) and were sacrificed 1 week later (n=5/group). Representative image showing cells expressing both the tdTomato and GFP reporters (arrows). 3V: 3rd ventricle, ME: median eminence. Scale bars: 50 µm.

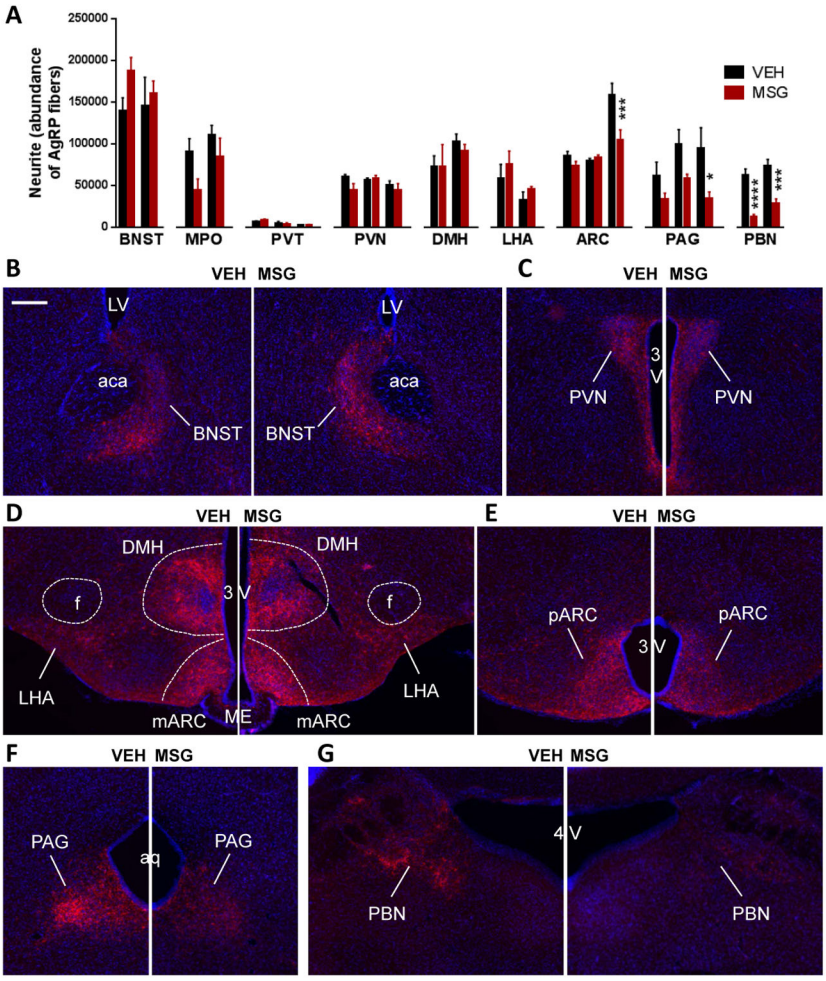


**Figure 6. MSG treatment led to reduction in AgRP-immunoreactive fibers innervating hindbrain targets**

4- to 6-month-old female mice received an injection of vehicle or MSG and examined 3 weeks later. **(A)** Quantification AgRP immunoreactive fibers and (**B–G**) representative sections showing AgRP projections in the (**B**) BNST, (**C**) PVN, (**D**) DMH, LHA, and medial ARC, (**E**) posterior ARC, (**F**) PAG, and (**G**) PBN in vehicle- and MSG-treated brains. Data are means ± SEM of n=4–5/group, * P<0.05, *** P<0.001, **** P<0.0001 as indicated by two-way ANOVA for each nucleus examined, followed by Sidak's multiple comparison tests. 3V: 3rd ventricle, 4V: 4$^{th}$ ventricle, aca: anterior commissure, Aq: Aqueduct, BNST: bed nucleus of the stria terminalis, DMH: dorsomedial hypothalamus, f: fornix, LHA: lateral hypothalamus, LV: lateral ventricle, mARC: medial arcuate nucleus, ME: median eminence, pARC: posterior arcuate nucleus, PAG: periaqueductal grey, PBN: parabranchial nucleus. Scale bar: 200 μm.

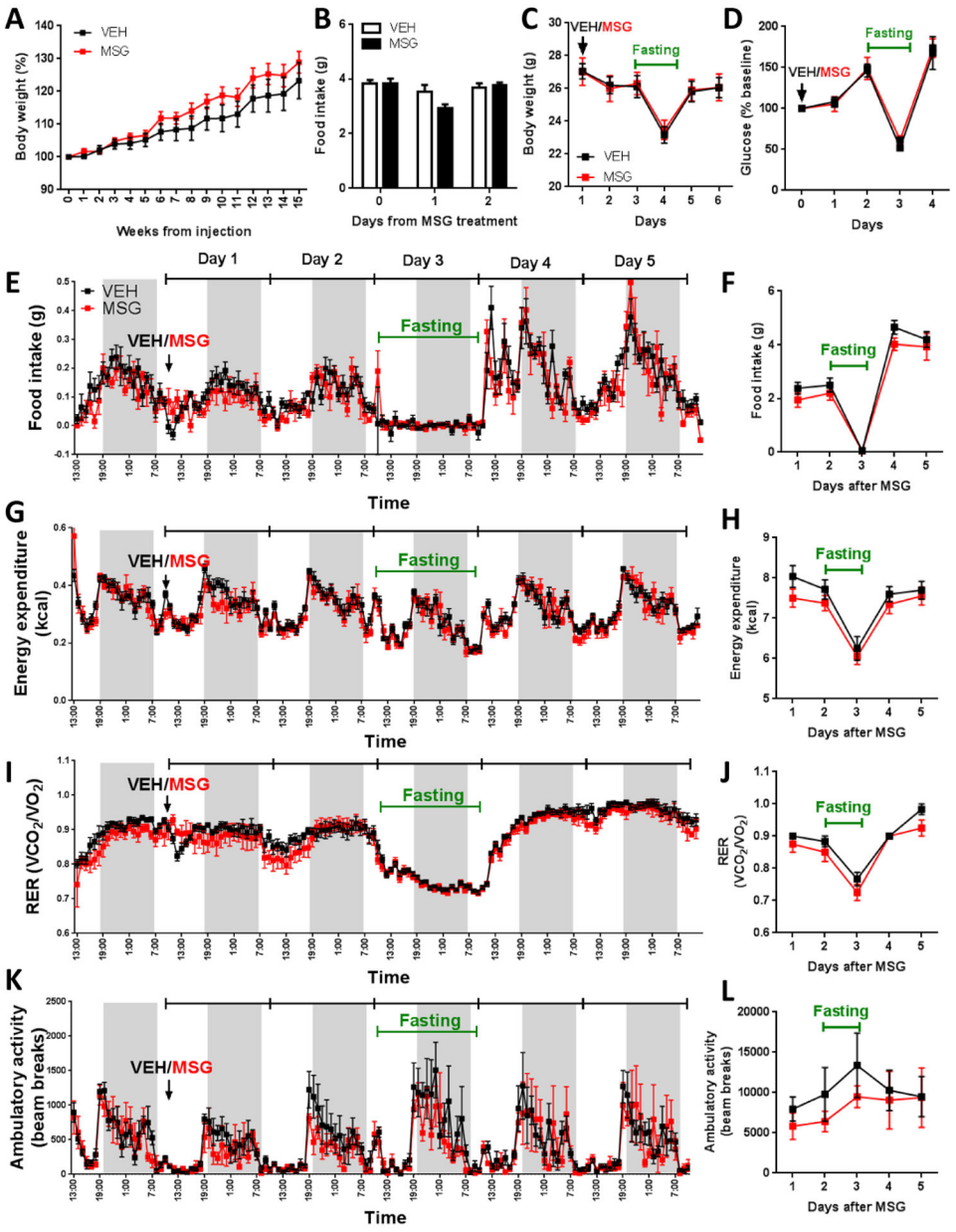


**Figure 7. Adult animals are able to maintain energy balance without any gross abnormality in response to MSG**

(**A**) 8- to 16-week-old mice were given an injection of vehicle or MSG and were monitored for up to 4 months. MSG-treated animals showed no reduction in body weight compared to vehicle-treated controls (n=7/group). (**B**) Mice showed a small and transient decrease in baseline food intake in the day following MSG treatment relative to controls (n=5–6/group). (**C**) Body weight response to a 24-hour period of fasting followed by refeeding were not different between animals treated acutely with vehicle or MSG (n=4–6/group). (**D**). Blood glucose level in vehicle- and MSG-treated animals under baseline condition and following a 24-hour fast (n=5–6/group). (**E–L**) CLAMS measurements were performed at 30°C. (**E**) Food intake during light and dark cycles and (**F**) total daily food intake. (**G**) Energy

expenditure during light and dark cycles and (**H**) total daily energy expenditure. (**I**) Respiratory exchange ratio (RER) during light and dark cycles and (**J**) average daily RER. (**K**) Ambulatory activities during light and dark cycles and (**L**) total daily ambulatory activities (n=4–6/group). Data are means ± SEM.